

University of Arkansas, Fayetteville

ScholarWorks@UARK

Chemical Engineering Undergraduate Honors
Theses

Chemical Engineering

12-2019

Effects of a double mutation in the heparin binding pocket on hFGF-1

Vanessa Weidling

Follow this and additional works at: <https://scholarworks.uark.edu/cheguht>

 Part of the [Amino Acids, Peptides, and Proteins Commons](#)

Recommended Citation

Weidling, Vanessa, "Effects of a double mutation in the heparin binding pocket on hFGF-1" (2019).
Chemical Engineering Undergraduate Honors Theses. 155.
<https://scholarworks.uark.edu/cheguht/155>

This Thesis is brought to you for free and open access by the Chemical Engineering at ScholarWorks@UARK. It has been accepted for inclusion in Chemical Engineering Undergraduate Honors Theses by an authorized administrator of ScholarWorks@UARK. For more information, please contact ccmiddle@uark.edu.

Effects of a double mutation in the heparin binding
pocket on hFGF-1

Vanessa Weidling

Undergraduate thesis submitted in partial requirements of honors studies in Chemical

Engineering

Fall 2019

Department of Chemistry and Biochemistry

University of Arkansas, Fayetteville

Acknowledgments

This project was supported by the Department of Energy (grant number DE-FG02-01ER15161), the National Institutes of Health/National Cancer Institute (NIH/NCI) (1 R01 CA 172631), the NIH through the COBRE program (P30 GM103450), and the Arkansas Biosciences Institute.

I would like to acknowledge the two graduate students who worked closely with me on this project, Julie Davis and Shilpi Agarwal. I would also like to thank Dr. Kumar my research mentor for guiding us through the twists and turns of research. He has encouraged and inspired me to continue research throughout my career. Additionally, this project wouldn't have been possible without the constant support of all the graduate students in the lab who answered all my many questions and helped me anytime I needed it. The Kumar lab has made my undergraduate research experience special and unforgettable.

Abstract

The human acidic fibroblast growth factor (hFGF-1) is a protein that plays an important role in many body processes such as angiogenesis and tissue repair. As such, it has great potential for therapeutic application. However, hFGF-1 is relatively unstable in the body with a significant fraction being denatured at body temperature and pH. It contains a group of positively charged amino acids in close proximity that create an electrostatic strain on the molecule and can lead to denaturation and increased susceptibility to enzymatic digestion. Upon its release from the cell, hFGF-1 binds to the glycosaminoglycan heparin in the extracellular matrix. Heparin stabilizes hFGF-1 by binding to this group of positively charged amino acids, known as the heparin binding pocket. Heparin also mediates the binding of hFGF-1 to cell surface FGF Receptors

(FGFRs). When activated by hFGF-1, these receptors propagate a signal downstream to initiate various pathways inside the cell. This study examines a mutation of hFGF-1 in which two negative charges are introduced into the heparin binding pocket. The introduction of these charges decreased the binding affinity of hFGF-1 for heparin by about 3-fold. This mutation also showed similar bioactivity compared to wild type hFGF-1 (wt-hFGF-1) both in the presence and absence of heparin. Overall, these results suggest that heparin binding affinity is not positively correlated with mitogenic activity. Additionally, it was shown that heparin binding is not necessary for activation of the tyrosine kinase cell surface receptor.

Introduction

The fibroblast growth factor family (FGFs) are a group of signaling molecules with a vast array of biological functions [1, 2]. They exhibit their effects by binding to various isoforms of 4 cell surface receptors or FGFRs [3, 4]. hFGF-1 can bind to and activate all FGFR isoforms, and as such it is a good choice for clinical applications [5]. One such application is wound healing.

Wound healing is generally divided into four stages: hemostasis, inflammation, proliferation, and remodeling [6]. During the third stage, proliferation, fibroblasts activated by FGFs proliferate epithelial cells and plug the wound with collagen [6]. This process begins several days to weeks after the injury [6]. This leaves the wound covered with only a blood clot before that time and relatively open to the environment. Because of this, during the first two phases of wound healing, the body is prone to infection. A serum containing hFGF-1 could be used to speed recovery from surgical incisions or other wounds, thereby lowering risk of infection [7]. It could also be used to treat slow healing chronic wounds in diabetes patients [7].

In the body, hFGF-1 binds to heparin sulfate, a glycosaminoglycan present in the extracellular matrix that serves to stabilize hFGF-1 during its binding to an FGFR [3]. Heparin binds to hFGF-1 via the heparin binding pocket, three surface loops that contain many positively charged amino acids near the c-terminal of the protein [8, 9]. Crystal structures of FGFR and hFGF-1 reveal that dimers formed both by receptors and growth factors seem to be mediated by heparin [10]. It is generally thought that heparin is necessary for FGFR activation [11].

Thrombin is an enzyme that is present at a wound site and can cleave hFGF-1 at position R136 [12]. A previous mutation studied by the Kumar lab of arginine at position 136 to glutamate showed a slight decrease in heparin binding affinity and a dramatic increase in stability and cell proliferation activity when compared to the wild type [13]. This study investigated whether the introduction of another negative charge, glutamate at position 135, in conjunction with an R136E mutation could further improve stability and cell proliferation activity. When two negative charges were introduced into the heparin binding pocket, the bioactivity was similar when compared to wild type both in the presence and absence of heparin. Additionally, the heparin binding affinity of the mutant was roughly 3 times lower than the wild type. Further study of mutations of proline at position 135 revealed that the single mutation of proline to glutamate at position 135 resulted in an increase in heparin binding affinity as compared to the wild type [13]. This suggests that the R136E mutation played a large role in the decreased heparin binding affinity of P135E/R136E [13]. Overall, these results show that the addition of the mutation P135E to the R136E mutation did not confer additional stability or bioactivity to the protein. However, an interesting finding was that mitogenic activity was not positively correlated with heparin binding affinity. Additionally, it was shown that heparin is helpful for providing stability

during hFGF-1-FGFR binding, but it is not strictly necessary for activation of an FGFR by hFGF-1.

Results and Discussion

Structural changes

hFGF-1 contains eight tyrosine residues and one tryptophan residue [14]. These aromatic amino acids can be used to identify the denatured state of the protein via intrinsic fluorescence. The tyrosine residues have a characteristic maximum fluorescence intensity at an emission wavelength of 308nm, while for tryptophan the maximum occurs at 350nm. hFGF-1 in its native state has a high intensity peak at 308nm and no peak at 350nm due to the quenching effect of the amino groups on the side chains which surround the tryptophan residue [15]. Its denatured state is determined by the presence of a large peak at 350nm due to the tryptophan residue shifting away from the quenching groups. Relative intrinsic fluorescence experiments were conducted to determine if the mutant appeared to be properly folded. The ratio of fluorescence values for 308nm/350nm was lower in the mutant than in wt-hFGF-1 both in the presence and absence of heparin (Figure 1). Without heparin, the double mutant had a ratio of 1.76 while for wt-hFGF-1 it was 7.20. With heparin, the double mutant had a ratio of 1.63 while for wt-hFGF-1, the ratio was 7.43. Although the ratio of 308/350nm was higher in the double mutant, than wt-hFGF-1, the characteristic fluorescence spectrum of the folded protein of a high peak at 308 and a drop thereafter is maintained. The increase in the ratio results from a broader shoulder in the double mutation around the wavelengths 320-380 nm. It is known that the indole side chain in W121 is quenched by the amino groups in the proline and lysine residues positioned nearby [15]. Additionally, W121 is positioned 3.5 Angstroms away from the pyrrole side chain of proline in

native hFGF-1 [15]. Therefore, with the substitution of glutamate at position 135, it is plausible that the indole group is shifted away from the other quenching groups, creating this shoulder.

Far UV Circular Dichroism (CD) is used to examine the secondary structure of proteins. The difference in the absorption of right and left circularly polarized light by the sample is used to calculate a value of molar ellipticity at various wavelengths. This can reveal patterns characteristic of alpha helices and beta sheets [16]. The CD data for the double mutant overlays well with wt-hFGF-1 (Figure 2). Both show the characteristic shape of a beta trefoil fold; a negative peak at 207nm and a positive peak at around 230nm. This indicates that the secondary structure is not significantly perturbed as a result of the mutation.

8-Anilinonaphthalene-1-sulfonic acid (ANS) is a fluorescent molecular probe used to test for the presence of hydrophobic residues on the surface of proteins [17]. An increase in the fluorescence of ANS is indicative of a higher presence of hydrophobic residues that are solvent accessible [17]. ANS was added in increments of 20 μM to a sample of protein and fluorescence measurements were taken at 500 nm from 0 μM ANS to 400 μM ANS. The fluorescence measured for P135E/R136E in the presence and absence of heparin did not significantly differ from wt-hFGF-1 (Figure 3). This indicates that the tertiary structure is not significantly perturbed due to the introduction of two negative charges in the heparin binding pocket. This result corroborates with the intrinsic fluorescence and the CD spectra for this mutation.

Nuclear magnetic resonance is a technique used to determine changes in the backbone arrangement of a protein. Its utility lies in its ability to give information about changes to specific residues [18]. Cells are grown in media with N^{15} , a radioactive isotope of nitrogen. Protein is then extracted using established laboratory techniques. The protein samples are exposed briefly to a magnetic field which aligns all of the H nuclei. Then, the magnetic field is removed and

nuclei are allowed to precess for a time, t_1 . During this time, the chemical shift of the H nucleus is labeled. Each proton attached to a heteronucleus (N15) produces a distinct peak in the spectrum. Then, magnetization is transferred to the second nucleus (N15), and the chemical shift of these nuclei is measured and labeled. Collectively, these can be combined to show the shift of each N15-H pair in each amino acid. If the spectra from two different samples are overlaid, the residues experiencing a change in conformation will experience a greater chemical shift and therefore will not overlap. The spectra for wt-hFGF-1 and P135E/R136E were overlaid (Figure 4). G134 is the most perturbed amino acid in the heparin binding pocket and T83, G85, and G89 are the most perturbed outside the heparin binding pocket. The proximity of these amino acids suggests that the structural changes due to the mutation are just local. This corroborates well with the other structural experiments.

Stability

The stability of the mutant under thermal stress was measured in the presence and absence of heparin. The mutant was heated from 25°C to 75°C in 5 degree increments while measuring the fluorescence at 308 and 350nm to detect unfolding of the protein. The T_m (temperature at which 50% of the protein in the sample is unfolded) for the mutant without heparin was 53°C, while for wt-hFGF-1 the T_m was 48.5 °C [15]. In the presence of heparin, the T_m for the double mutant was 57.7 °C while for wt-hFGF-1, the T_m is much higher, 69.0 °C [15]. The ΔT_m value for P135E/R136E is 4.7 °C, while the ΔT_m for wt-hFGF-1 is 20.5 °C[15]. Comparing the ΔT_m values illustrates that the mutant is not as stabilized by heparin as the wild type. This is likely due to the lower binding affinity of the mutant for heparin. Additionally, this mutation is slightly more thermally stable than wt-hFGF1 in the absence of heparin.

Urea is a denaturing agent that can disrupt intramolecular hydrogen bonds and lead to denaturation of a protein [19]. Urea was titrated in to the protein samples from 0M to 6M and the fluorescence values at 308 and 350 nm were monitored to determine when the protein was unfolded (Figure 5). The mutant alone showed a C_m (the concentration at which half of the protein is denatured) of 1.76 M. This is close to wt-hFGF1, which has a C_m of 1.81 M. For the mutant, the C_m in the presence of heparin was 2.27 M while for wt-hFGF1, the C_m is 4.18. The ΔC_m for the mutant and wild type are 0.5 M and 1.91 respectively. The stability of the mutant is similar to wt-hFGF-1 in the absence of heparin. In the presence of heparin, the mutant is not stabilized to the same degree as wt-hFGF-1 and is much more susceptible to denaturation by urea. This is again likely due to the fact that the mutant has a lower binding affinity to heparin than the wild type does.

Heparin binding affinity

Isothermal titration calorimetry (ITC) is used to measure the thermodynamic properties of the interaction between a protein and its ligand [20]. ITC was used to detect heat changes that occurred when heparin was injected into both a sample of hFGF-1 and P135E/R136E (Figures 6 and 7). This was done by measuring the power required to maintain a temperature difference of zero between the sample cell containing protein and the reference cell containing buffer, both contained in an insulated, adiabatic system. The dissociation constant (K_d) and the change in enthalpy (ΔH) can also be measured using ITC.

The dissociation constant (K_d) of the mutant for heparin was increased as compared to the wild type: $K_d = 4.6\mu\text{M}$ and $K_d = 1.7\mu\text{M}$ respectively. Therefore, the heparin binding affinity was decreased for the mutant. In examining other mutations, it was found that substituting just one

negative charge at position 135 (P135E) actually increased heparin binding affinity ($K_d = 0.58\mu\text{M}$) [15]. Therefore, the mutation at position 136 likely has a large role in the decrease in heparin binding affinity of P135E/R136E [15]. The change in enthalpy was also measured. The change in enthalpy for the mutant was $\Delta H = -0.85 \text{ kcal/mol}$ [15]. The magnitude of this change was smaller than the wild type ($\Delta H = -2.14 \text{ kcal/mol}$) [15]. This indicates that there is not as much contact between the mutant and heparin as compared to the heparin-wt-hFGF-1 interaction [15].

Bioactivity

To measure cell proliferation, NIH3T3 (human fibroblast) cells treated with heparinase (to remove the heparin from the cell surface) were grown in a culture with the hFGF-1 mutant and wild type in the presence and absence of heparin (Figures 8 and 9). Cell number was measured after 24 hours. The double mutant showed a similar bioactivity to wt-hFGF1 both in the presence and absence of heparin. Without heparin, the bioactivity of the mutant is slightly higher at higher concentrations of protein (10 and 50 ng/mL) than wt-hFGF-1. Upon the addition of heparin, the bioactivity of the mutant and the wild type are the same.

Conclusions

Overall, this study shows that while heparin increases the bioactivity of both wt-hFGF-1 and P135E/R136E, a decrease in heparin binding affinity did not negatively affect cell proliferation activity of the mutant. Additionally, it can be said that heparin is not strictly required for hFGF-1 to activate a cell surface receptor. The addition of a negative charge at position 135 to the R136E mutation did not confer additional stability or cell proliferation activity to hFGF-1. These results

can direct further study of this protein with the goal of increasing stability and bioactivity of the protein for applications in wound healing.

Materials and Methods

Materials

Primers were designed using Agilent primer design software, IDT DNA Inc, USA. Plasmid isolation was accomplished using kits from Qiagen USA. Site directed mutagenesis kits were purchased from Agilent. DH5a and BL-21 competent cells (*Escherichia coli*) were from Novagen Inc, USA. Lysogeny Broth (LB) was from EMD Milipore, USA. Heparin sephrose for the purification column was from GE Healthcare. All buffer components: (Na_2HPO_4 , NaH_2PO_4 , NaCl , $(\text{NH}_4)\text{SO}_4$) were obtained from VWR Scientific Inc, USA. Low molecular weight heparin sodium salt used in experiments (molecular weight ~3kDa) was from Sigma and MP Biomedicals LLC. NIH3T3 cells were from American Type Culture Collection. DMEM media, fetal bovine serum, and penicillin streptomycin used for bioactivity experiments were all from Thermo Fisher Scientific.

Site directed mutagenesis and bacterial transformation

pET20b bacterial expression vector was the template for site directed mutagenesis. Instructions for the QuikChange II XL kit were followed for SDM. The heat shock method was used to transform the plasmid into the DH5a competent cells, and the sequence was verified by UAMS. Overexpression of the mutant was then carried out using BL-21 competent cells. The cells were incubated overnight in LB media at 37°C. IPTG was added after an optical density (measured by Hitachi F-2500 spectrofluorometer) of 0.4-0.6 was reached. After overexpression, cells were lysed using sonication, and protein was separated by centrifugation for 1 hour at 19,000 rpm. No post

translational modifications are known to occur in hFGF-1 [15]. Purification was carried out using a heparin sephrose resin column. Buffers with 10mM phosphate (Na_2HPO_4 , NaH_2PO_4) and 25mM ammonium sulfate ($(\text{NH}_4)\text{SO}_4$) and pH of 7.2 with increasing NaCl concentrations were loaded into the column to elute the protein. wt-hFGF-1 eluted at 1500mM NaCl and the mutant eluted at 800mM NaCl. The presence of protein was determined by SDS-PAGE analysis with a standard protein marker. Concentrations were determined using the Bradford assay with a Hitachi F-2500 Fluorimeter. All protein samples were prepared using a 1:10 mole ratio of protein to heparin as this was found to achieve maximum cell proliferation activity.

Structural Experiments

Fluorescence and ANS experiments were performed on a Hitachi F-2500 fluorimeter at 25°C with a slit width set to 2.5 nm. For fluorescence experiments, a quartz cuvette with path length of 1 cm was used with protein concentration of 1 mg/mL. An excitation wavelength of 280nm and emission wavelength range of 300-450nm were used. For the ANS assay, 1 μL of 20mM stock ANS was added to the sample before each measurement to increase the concentration of ANS by 20 μM increments. With each addition, the fluorescence value was measured at 500 nm.

Far-UV CD was performed on a Jasco 1500 spectropolarimeter. A protein concentration of 0.5mg/mL was used at 25°C. A sandwich cuvette used with path length 0.1 cm.

For 2-D NMR a Bruker 500MHx NMR was used with a cryoprobe. A protein concentration of 5mg/mL in 10mM PB (Na_2HPO_4 , NaH_2PO_4), 100mM NaCl, 25mM $(\text{NH}_4)\text{SO}_4$, and a pH of 7.2 at 25°C was used. Data was analyzed using Sparky 3.114 software. Chemical shift was calculated using the formula $\sqrt{[(2\Delta\delta\text{NH})^2 + (\Delta\delta\text{N})^2]}$.

Stability Experiments

Thermal and chemical denaturation experiments were performed using a Jasco-1500 spectropolarimeter, with a protein concentrations of 0.5mg/mL in 10mM PB (Na_2HPO_4 , NaH_2PO_4), 100mM NaCl, 25mM $(\text{NH}_4)\text{SO}_4$, at a pH of 7.2. For thermal denaturation, the fraction unfolded was calculated using $(F_x - F_{20})/(F_{80} - F_{20})$ where F is the fluorescence value at 308nm divided by the fluorescence value at 350nm and F_{20} and F_{80} are the fluorescence fractions at 20°C and 80°C respectively. For urea denaturation, urea was steadily added to increase the urea concentration from 0M to 6M and at each addition, the fluorescence value at 308nm and 350nm was recorded. The ratio of 308nm to 350nm was recorded and the fraction unfolded was calculated using $(F_x - F_0)/(F_6 - F_0)$. F is the fluorescence value at 308nm divided by the fluorescence value at 350nm and F_0 and F_6 are the fluorescence fractions at 0M urea and 6M urea respectively.

Heparin Binding Affinity

Heparin binding affinity was determined using ITC-200, Malvern Inc. Changes in heat were determined by titrating heparin into the reaction vessel containing the protein sample. Protein samples of 0.85mg/mL were made using 100mM NaCl and 25mM $(\text{NH}_4)\text{SO}_4$ at a pH of 7.2. The samples were degassed prior to titration. 30 titrations were performed at 25°C and 1000 rpm stir speed. Corrections were applied to adjust for the heats of dilution.

Cell Proliferation

For cell proliferation experiments, NIH3T3 fibroblast cells from ATCC were cultured in DMEM with 10% FBS, 1% penicillin/streptomycin. When 80%-90% confluency was reached, the cells were incubated overnight in serum-free media at 37°C with 5% carbon dioxide. Heparin on the cell

surface was removed by adding heparinase (6 units to 10,000 cells). After washing cells with PBS, they were returned to DMEM. Heparin was then added in a 1:10 protein to heparin ratio. Cells were divided into wells with 10,000 cells per well. Protein was added to different cells at concentrations of 0, 0.4, 2, 10, and 50 ng/mL and then incubated for one day (24 hours). Then, the CellTiter-Glo (Promega, Madison, WI) cell proliferation assay was used to determine the quantity of NIH3T3 cells.

Legend to Figures

All experiments were conducted using a ratio of 1:10 protein to heparin. Protein samples were prepared in 10mM PB (Na_2HPO_4 , NaH_2PO_4), 100mM NaCl, 25mM $(\text{NH}_4)\text{SO}_4$, at a pH of 7.2.

All experiments with the exception of thermal denaturation and bioactivity were performed at 25°C. Bioactivity experiments were performed at 37°C and thermal denaturation experiments were performed in the range of 25°C-75°C.

Figure 1: A protein concentration of 1mg/mL was used. Relative fluorescence is shown on the y-axis at wavelengths from 300-450nm (shown on the x-axis).

Figure 2: A protein concentration of 0.5mg/mL was used. Molar ellipticity is shown on the y-axis at various wavelengths (shown on the x-axis).

Figure 3: A protein concentration of 0.25mg/mL was used. Fluorescence at 500nm is shown on the y-axis and concentration of ANS is shown on the x-axis.

Figure 4: A protein concentration of at least 5mg/mL was used. Chemical shift for hydrogen is shown on the x-axis and chemical shift for nitrogen is shown on the y-axis. The mutant is labeled red and the wild type is labeled blue.

Figure 5: Protein samples were prepared with a protein concentration of 0.5mg/mL. Urea was titrated in from 0M to 6M urea and the fluorescence values at 308nm and 350nm were recorded to determine when the protein unfolded. The fraction of protein unfolded is shown on the y-axis.

Figure 6 and 7: A protein concentration of 0.85mg/mL was used. The power requirement for the sample and reference cell to remain at the same temperature is shown in the upper portion of the graph. The energy change when heparin was added is shown in the bottom portion. The K_d (dissociation constant) is also displayed on the bottom portion of the graph.

Figures 8 and 9: Protein concentrations are indicated by the different colored bars (refer to the legend at bottom of the graph) and the cell number is displayed on the y-axis. The proteins involved in this thesis are circled.

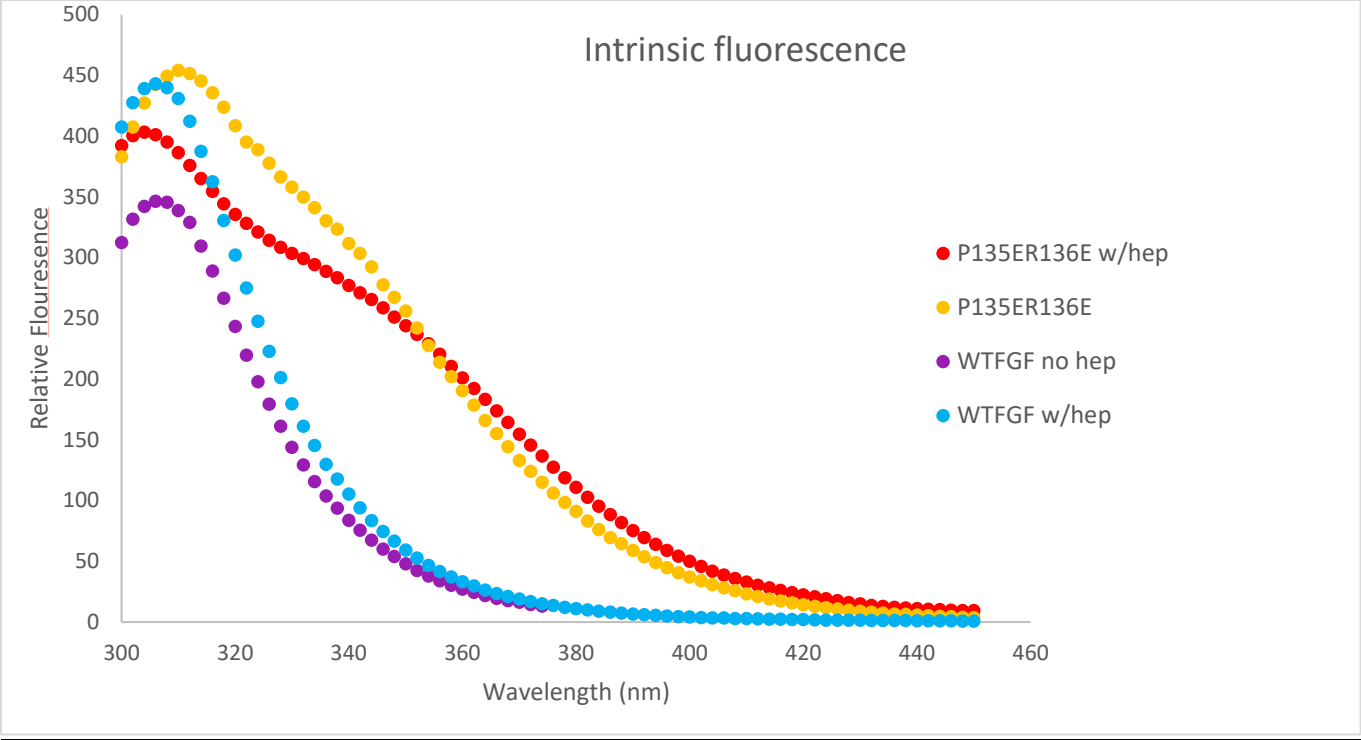


Figure 1. Intrinsic Fluorescence.

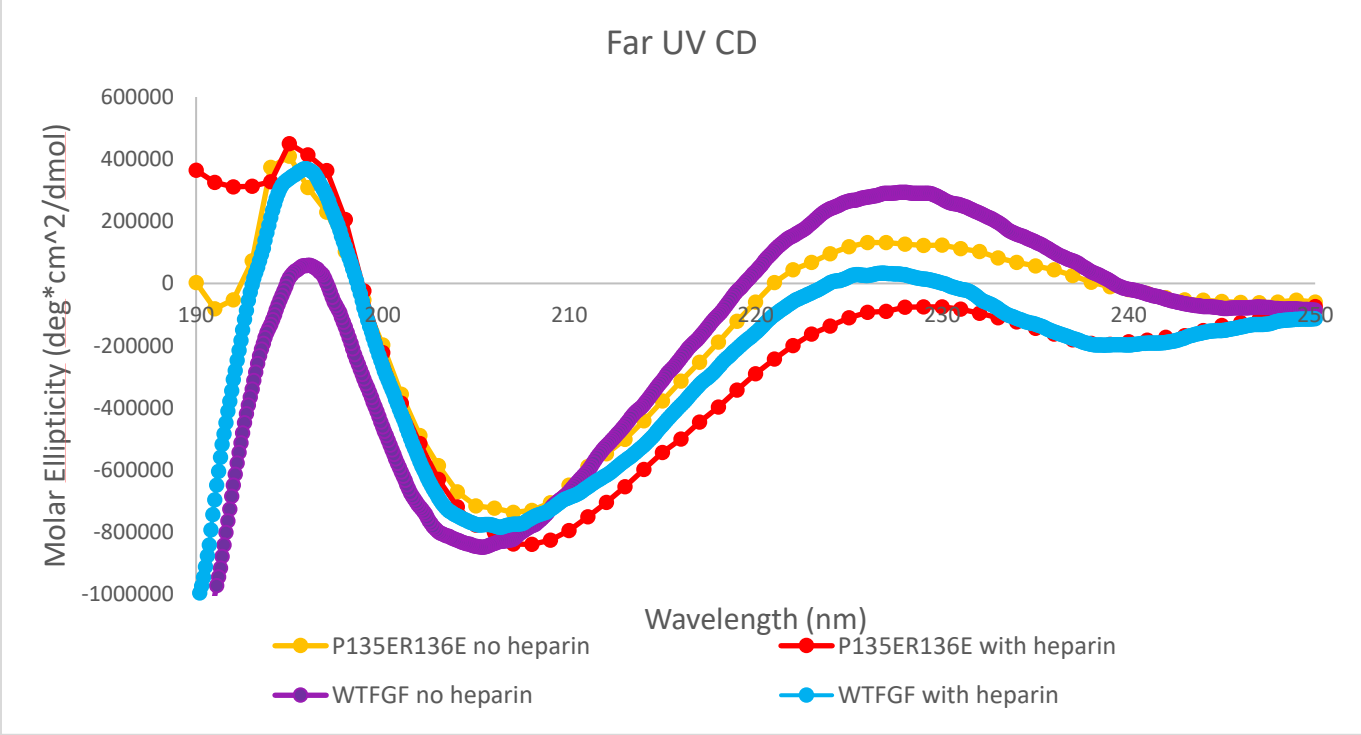


Figure 2. Far UV Circular Dichroism.

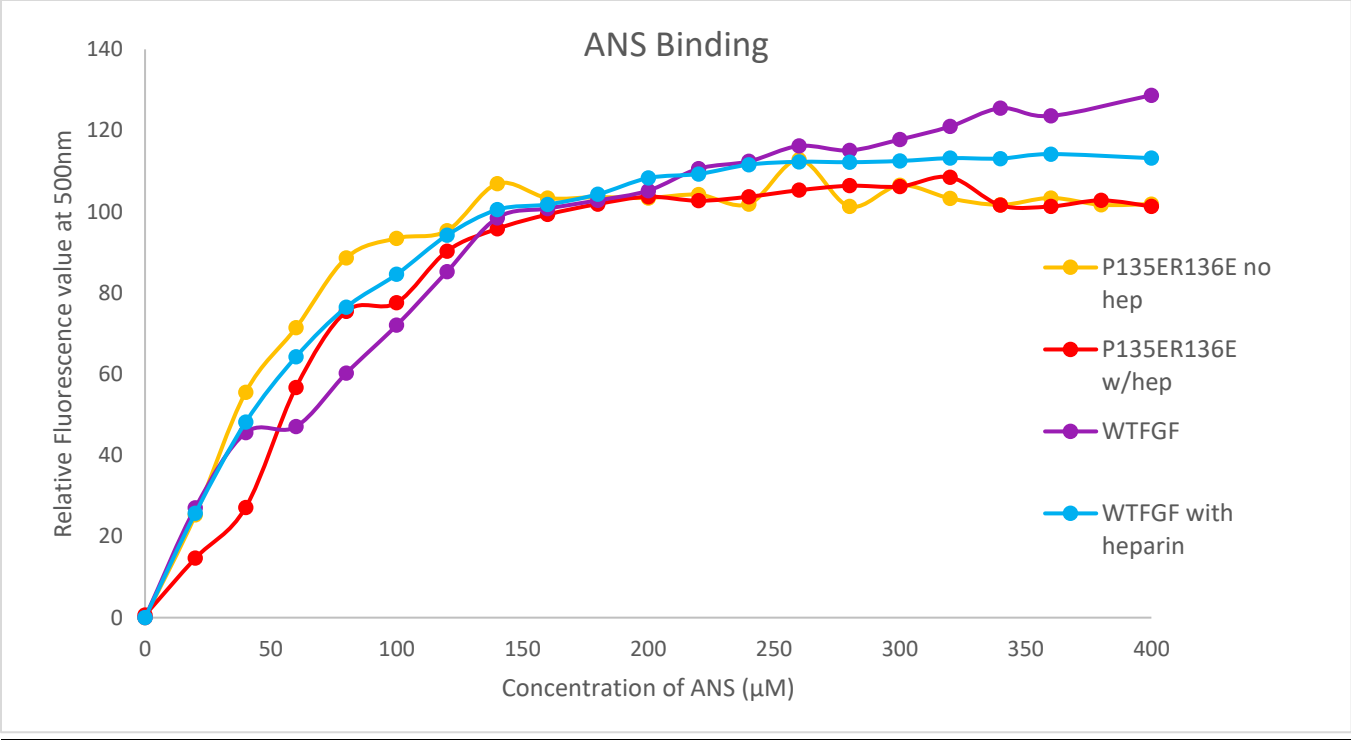


Figure 3. ANS Binding.

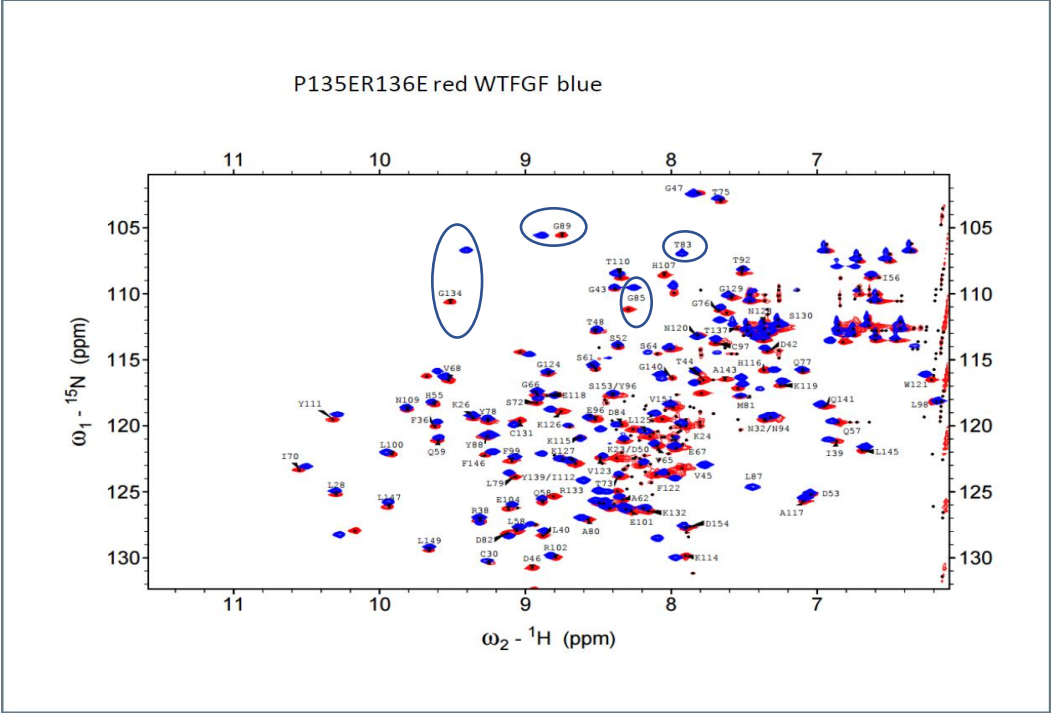


Figure 4. NMR Spectra.

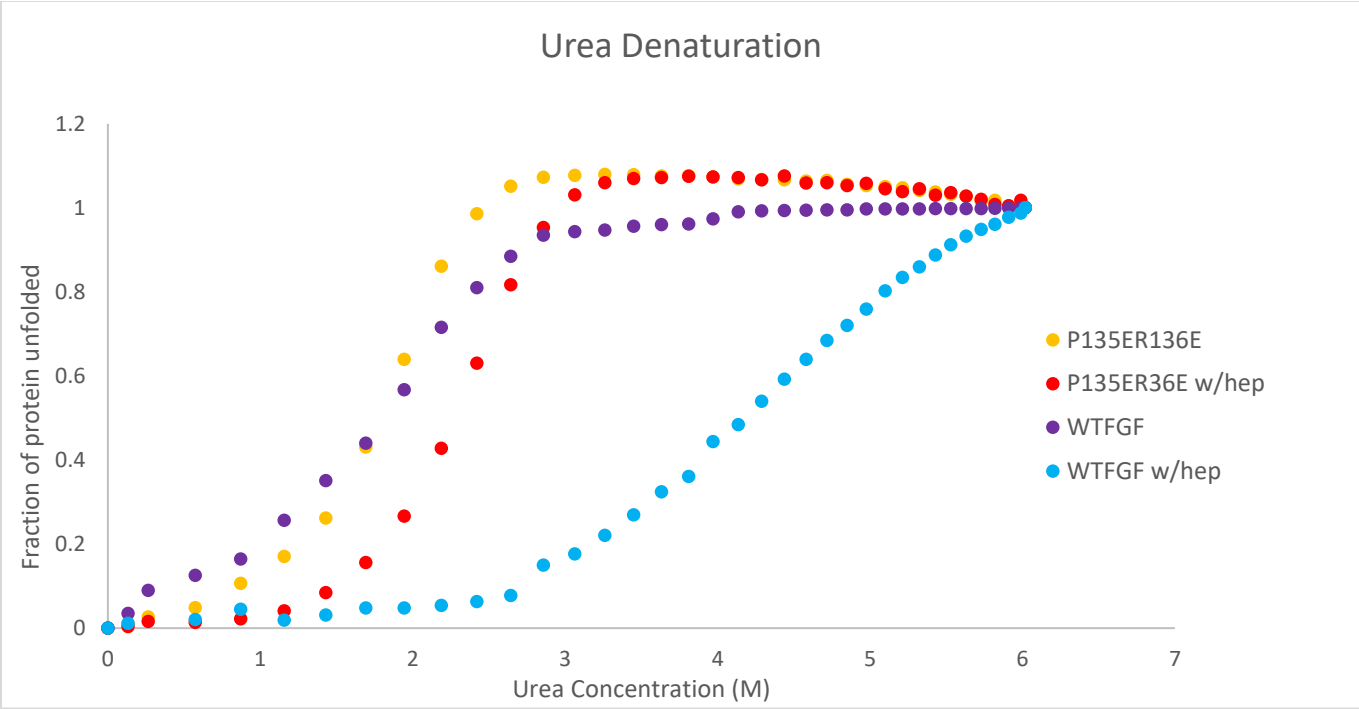
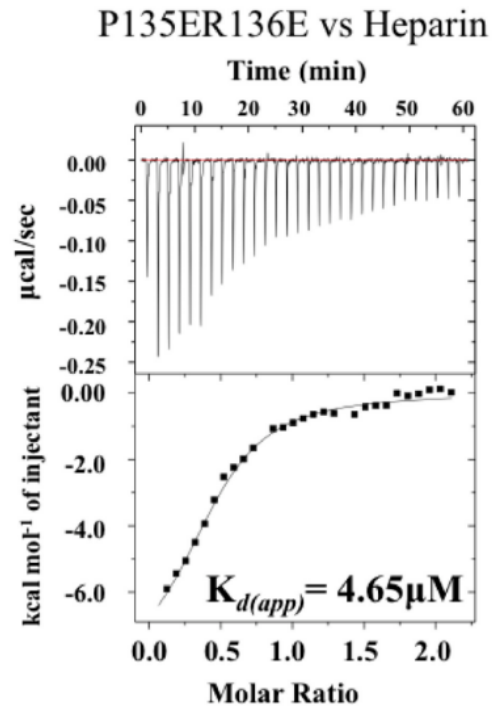
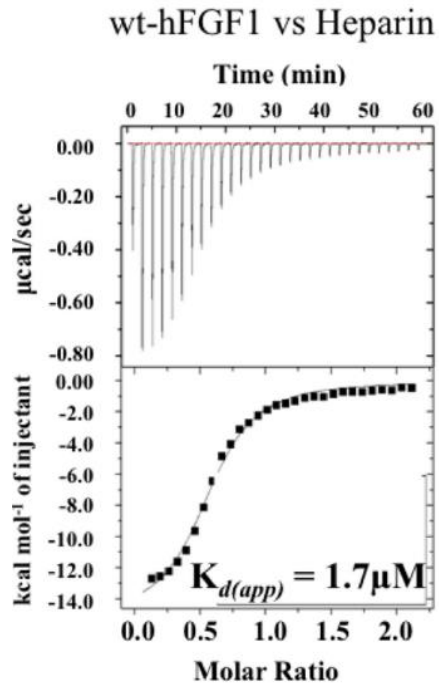


Figure 5. Urea Denaturation.



Figures 6 and 7. ITC data for wt-hFGF-1. Reproduced from Julie Davis et al, *Probing the Role of Proline 135 on the Structure, Stability and Cell Proliferation Activity of Human Acidic Fibroblast Growth Factor*. Archives of Biochemistry and Biophysics, 2018, volume 654, pages 115-125.

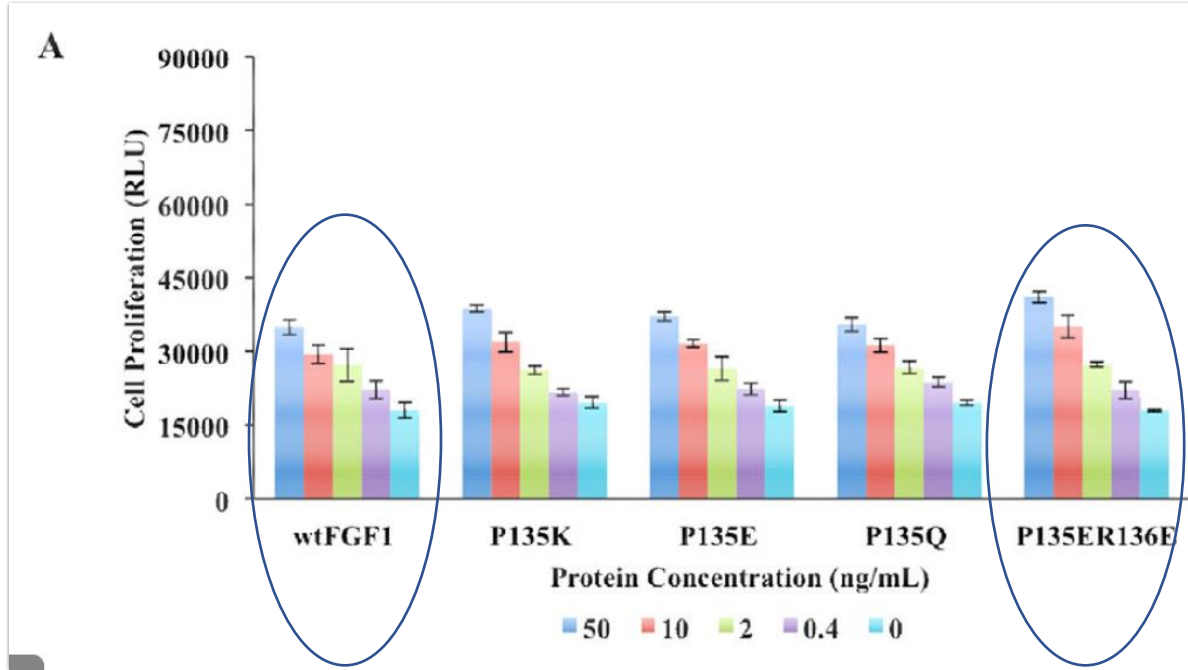


Figure 8. Bioactivity data (without heparin). Reproduced from Julie Davis et al, *Probing the Role of Proline 135 on the Structure, Stability and Cell Proliferation Activity of Human Acidic Fibroblast Growth Factor*. Archives of Biochemistry and Biophysics, 2018, volume 654, pages 115-125.

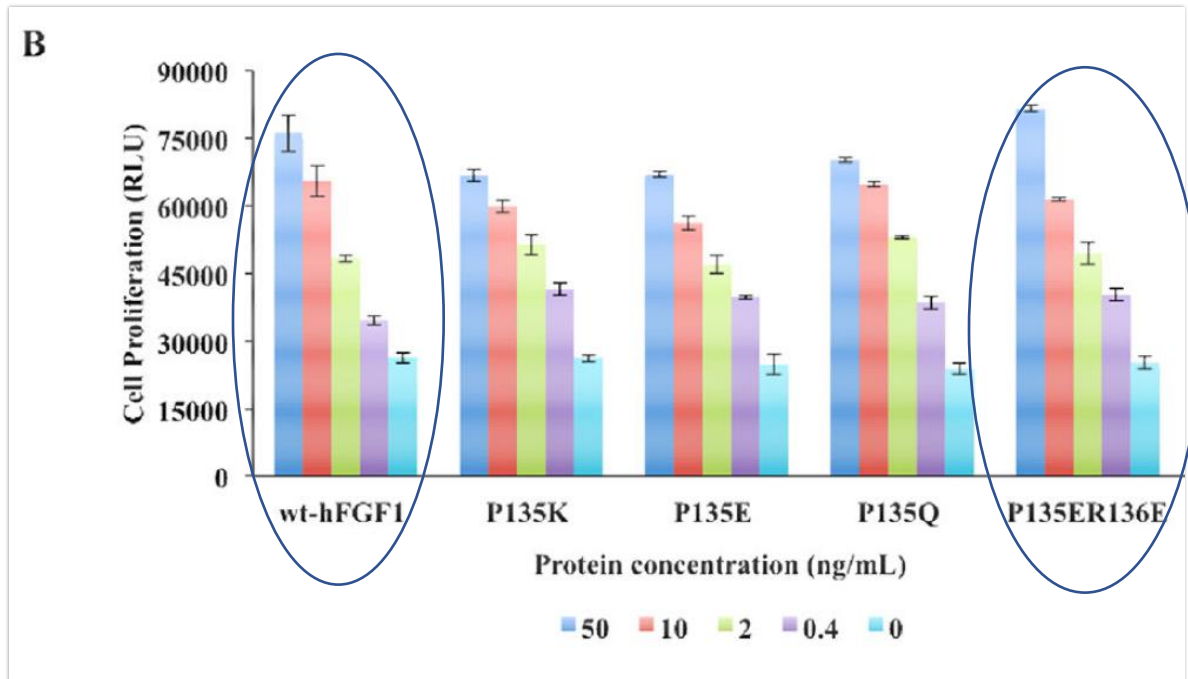


Figure 9. Bioactivity data (with heparin). Reproduced from Julie Davis et al, *Probing the Role of Proline 135 on the Structure, Stability and Cell Proliferation Activity of Human Acidic Fibroblast Growth Factor*. Archives of Biochemistry and Biophysics, 2018, volume 654, pages 115-125.

References

1. FGF1 fibroblast growth factor 1 [Homo sapiens (human)] - Gene - NCBI. (n.d.). Retrieved from <https://www.ncbi.nlm.nih.gov/gene?Db=gene&Cmd=ShowDetailView&TermToSearch=2246>.
2. Beenken, A., & Mohammadi, M. (2009). The FGF family: biology, pathophysiology and therapy. *Nature Reviews Drug Discovery*, 8(3), 235–253. doi: 10.1038/nrd2792
3. Britt-Marie Loo, J. K. (2001). Binding of Heparin Sulfate to Fibroblast Growth Factor Receptor 4. *Journal of Biological Chemistry*.
4. Belov, A. A., & Mohammadi, M. (2013). Molecular Mechanisms of Fibroblast Growth Factor Signaling in Physiology and Pathology. *Cold Spring Harbor Perspectives in Biology*, 5(6). doi: 10.1101/cshperspect.a015958
5. Xiuqin Zhang, O. I. (2006). Receptor Specificity of the Fibroblast Growth Factor Family. *Journal of Biological Chemistry*, 15694-15700.
6. Post-Operative Surgical Wound Management: Key Wound Treatment Considerations. (2018, October 10). Retrieved from <https://www.woundsource.com/blog/post-operative-surgical-wound-management-key-wound-treatment-considerations>.
7. Demidova-Rice, T. N., Hamblin, M. R., & Herman, I. M. (2012). Acute and Impaired Wound Healing. *Advances in Skin & Wound Care*, 25(8), 349–370. doi: 10.1097/01.asw.0000418541.31366.a3
8. Brown, A., Robinson, C. J., Gallagher, J. T., & Blundell, T. L. (2013). Cooperative Heparin-Mediated Oligomerization of Fibroblast Growth Factor-1 (FGF1) Precedes Recruitment of FGFR2 to Ternary Complexes. *Biophysical Journal*, 104(8), 1720–1730. doi: 10.1016/j.bpj.2013.02.051
9. Wong, P., Hampton, B., Szylobryt, E., Gallagher, A. M., Jaye, M., & Burgess, W. H. (1995). Analysis of Putative Heparin-binding Domains of Fibroblast Growth Factor-1: Using site-directed mutagenesis and peptide analogues. *Journal of Biological Chemistry*, 270(43), 25805–25811. doi: 10.1074/jbc.270.43.25805
10. Pellegrini, L., Burke, D. F., Delft, F. V., Mulloy, B., & Blundell, T. L. (2000). Crystal structure of fibroblast growth factor receptor ectodomain bound to ligand and heparin. *Nature*, 407(6807), 1029–1034. doi: 10.1038/35039551
11. Harmer, N. (2006). Insights into the role of heparan sulphate in fibroblast growth factor signalling: Figure 1. *Biochemical Society Transactions*, 34(3), 442–445. doi: 10.1042/bst0340442
12. Erzurum, V. Z., Bian, J.-F., Husak, V. A., Ellinger, J., Xue, L., Burgess, W. H., & Greisler, H. P. (2003). R136K fibroblast growth factor-1 mutant induces heparin-independent migration of endothelial cells through fibrin glue. *Journal of Vascular Surgery*, 37(5), 1075–1081. doi: 10.1067/mva.2003.177
13. Davis Eberle, Julie, "Engineering the Structure of the Human Acidic Fibroblast Growth Factor to Enhance its Stability and Cell Proliferation Activity" (2018). Theses and Dissertations. 2663.
14. Canales, Lozano, Angulo, Ojeda, & Nieto. (n.d.). Solution NMR structure of a human FGF-1 monomer, activated by a hexasaccharide heparin-analogue. Retrieved from <https://www.rcsb.org/structure/2ERM>.

15. Davis, J. E., Alghanmi, A., Gundampati, R. K., Jayanthi, S., Fields, E., Armstrong, M., ... Kumar, T. K. S. (2018). Probing the role of proline –135 on the structure, stability, and cell proliferation activity of human acidic fibroblast growth factor. *Archives of Biochemistry and Biophysics*, *654*, 115–125. doi: 10.1016/j.abb.2018.07.017
16. Whitmore, L., & Wallace, B. A. (2008). Protein secondary structure analyses from circular dichroism spectroscopy: Methods and reference databases. *Biopolymers*, *89*(5), 392–400. doi: 10.1002/bip.20853
17. Hawe, A., Sutter, M., & Jiskoot, W. (2008). Extrinsic Fluorescent Dyes as Tools for Protein Characterization. *Pharmaceutical Research*, *25*(7), 1487–1499. doi: 10.1007/s11095-007-9516-9
18. (n.d.). Retrieved from <http://www.cryst.bbk.ac.uk/PPS2/projects/schirra/html/2dnmr.htm>.
19. Bennion, B. J., & Daggett, V. (2003). The molecular basis for the chemical denaturation of proteins by urea. *Proceedings of the National Academy of Sciences*, *100*(9), 5142–5147. doi: 10.1073/pnas.0930122100
20. Dutta, A. K., Rösger, J., & Rajarathnam, K. (2014). Erratum: Using Isothermal Titration Calorimetry to Determine Thermodynamic Parameters of Protein–Glycosaminoglycan Interactions. *Methods in Molecular Biology Glycosaminoglycans*. doi: 10.1007/978-1-4939-1714-3_48